MRCI Calculations of the Lowest Potential Energy Surface for CH_3OH and Direct ab Initio Dynamics Simulations of the $O(^1D) + CH_4$ Reaction†

Hua-Gen Yu‡ and James T. Muckerman*

Department of Chemistry, Brookhaven National Laboratory, Upton, New York 11973-5000

Received: January 26, 2004; In Final Form: June 7, 2004

The stationary point geometries and frequencies on the lowest singlet potential energy surface for the CH_3OH system are calculated using the complete-active-space self-consistent-field method. The energetics are refined using a restricted internally contracted multireference configuration interaction (MRCI) method at the complete basis set (CBS) limit. The CBS energy is extrapolated using the scheme of Halkier et al. with two large basis sets: aug-cc-pVDZ and aug-cc-pVTZ. The implications of our calculated results concerning the $O(^1D) + CH_4$ and $OH + CH_3$ reactions are discussed. In addition, the $O(^1D) + CH_4$ reaction at a collision energy of 6.8 kcal/mol is investigated using a variant of the "scaling all correlation" (SAC) method of Truhlar et al. and the coupled-cluster double-excitation (CCD) method in a direct dynamics study with a D95(d,p) basis set. The results show that the $O(^1D) + CH_4 \rightarrow OH + CH_3$ reaction occurs both via direct and long-lived intermediate pathways. The differential cross section for the direct reaction to form OH is forward peaked with a nearly isotropic background. Finally, the branching fractions for OH, H, H_2, and H_2O are predicted to be 0.725:0.186:0.025:0.064.

I. Introduction

The reaction of methyl radicals with hydroxyl radicals is an important reaction in the combustion of hydrocarbons.[1−3] The reaction has eight possible product channels:

$$OH + CH_3 \rightarrow O(^1D) + CH_4, \quad \Delta H^0_{0K} = 39.53\text{kcal/mol} \quad (1)$$

$$\rightarrow 2H + H_2CO, \Delta H^0_{0K} = 33.51\text{kcal/mol} \quad (2)$$

$$\rightarrow H + CH_3O, \Delta H^0_{0K} = 13.53\text{kcal/mol} \quad (3)$$

$$\rightarrow H + CH_2OH, \quad \Delta H^0_{0K} = 4.2\text{kcal/mol} \quad (4)$$

$$\rightarrow CH_2(a\ ^1A_1) + H_2O, \quad \Delta H^0_{0K} = 0.77\text{kcal/mol} \quad (5)$$

$$\rightarrow H_2 + \textit{cis/trans}\text{-HCOH}, \quad \Delta H^0_{0K} = -16.19\text{kcal/mol} \quad (6)$$

$$\rightarrow H_2 + H_2CO, \Delta H^0_{0K} = -70.7\text{kcal/mol} \quad (7)$$

$$\rightarrow CH_3OH, \quad \Delta H^0_{0K} = -98.54\text{kcal/mol} \quad (8)$$

where reaction 5 is the dominant channel above room temperature.[1,4,5] Since these reactions occur via an intermediate CH_3OH without any barrier in the entrance channel of the ground-state potential energy surface, the measured rate constants are highly pressure-dependent, e.g., see ref 6 and references therein. Theoretically, by taking advantage of the deep well on the ground potential energy surface, several groups[6−8] have applied the variational RRKM (Rice−Ramsperger−Kassel−Marcus) theory to study these reactions. However, the statistical simulation strongly depends on the parameters used. In particular, the results are very sensitive to the endothermicity of the $CH_2(a^1A_1) + H_2O$ products.[8]

In addition, the $O(^1D) + CH_4$ reaction is a central reaction in the upper atmosphere. Although there are at least six possible product channels, the products are dominated by $OH + CH_3$ (69%).[9,10] The experimental results show that the $O(^1D) + CH_4 \rightarrow OH + CH_3$ reaction may proceed via multiple dynamical pathways.[9,11] In contrast, only an insertion pathway forming an intermediate complex can lead to the H, H_2, and H_2O products because they cannot be formed via the direct abstraction of a hydrogen atom. The interaction potential energy surface between $O(^1D)$ and methane in the entrance channel has been studied in detail by Arai[12] using a MRDCI method. A small barrier (2.1 kcal/mol) at a collinear O−H−C geometry was found. Recently, this small barrier was confirmed by Gonzalez and coworkers[10,13−15] using a PUMP4 theory, and they have also performed a quasi-classical trajectory dynamics study of the $O(^1D) + CH_4 \rightarrow OH + CH_3$ reaction using a pseudotriatomic PUMP4//UMP2 potential energy surface. Recently, they[16] also carried out a CASPT2 study of the two lowest singlet potential energy surfaces of the $O(^1D) + CH_4$ reaction system. Furthermore, the variational RRKM rate constants of Chang and Lin[17] suggest a nonstatistical behavior for the $OH + CH_3$ products in this reaction because it is so fast. Currently, there is no dynamics calculation available based on a realistic full-dimensionality potential energy surface for CH_3OH.

Although there are several accurate ab initio calculations[4,6,12−18] for the CH_3OH system, those studies addressed only the $O(^1D) + CH_4$ reaction,[12−17] the $OH + CH_3$ reaction,[4,6] or the decomposition of CH_3OH.[6,18] This is partly due to the difficulty in meeting the challenge of balancing the correlation energy for the wide variety of bond forming and breaking in the CH_3OH system. In this work, we attempt to study this system

† Part of the "Gert D. Billing Memorial Issue".

* Corresponding author. E-mail: muckerma@bnl.gov. Fax:+1-631-344 5815.

‡ E-mail: hgy@bnl.gov.

10.1021/jp049642p CCC: $27.50
Published on Web 08/12/2004

completely using a multireference ab initio method. For the $O(^1D) + CH_4$ reaction, a full-dimensionality direct ab initio dynamics study is carried out to understand the detailed reaction mechanism. As a result, the branching ratios of a variety of products can be computed. In contrast, the previous QCT dynamics studies[10,13−15] using a pseudotriatomic model allow only the $OH + CH_3$ product channel to be considered.

II. Computational Method

The potential energy surface for the CH_3OH system is explored by two electronic structure methods: the complete active space (CAS) SCF method, and the restricted internally contracted multireference CI (MRCI) method. The optimized geometries and harmonic frequencies of the reactants, transition states, intermediates, and products on the lowest singlet potential energy surface are calculated at the CAS(10,10)/cc-pVDZ level. That is, there are 10 active electrons and 10 active orbitals in the CASSCF study. The four inactive orbitals correlate to the core (1s) and the lowest valence (2s) orbitals of the carbon and oxygen atoms. All other valence orbitals are included in the active space. The energy of each stationary point is refined at the CAS(10,10)/cc-pVDZ optimized geometry by the restricted MRCI method with a large aug-cc-pVTZ basis set. The Davidson correlation energy correction is also included. These results are denoted as MRCI+Q/aug-cc-pVTZ//CAS(10,10)/cc-pVDZ. Similarly, the MRCI+Q/aug-cc-pVDZ// CAS(10,10)/cc-pVDZ energy for each point is also calculated. By using the extrapolation method of Halkier et al.,[19] the final energy (denoted as MRCI+Q/CBS) at the complete basis set (CBS) limit is given by

$$E_{\mathrm{MRCI+Q/CBS}} = E_{\mathrm{MRCI+Q/aug-cc-pVTZ}} + \frac{8}{19}(E_{\mathrm{MRCI+Q/aug-cc-pVTZ}} - E_{\mathrm{MRCI+Q/aug-cc-pVDZ}}) \quad (9)$$

In the restricted MRCI calculations, we have included in the reference function only those CAS configurations having no more than a total of two electrons in active space orbitals that are unoccupied in the principal ground-state configuration. The restricted reference functions nevertheless include all single and double excitations from the principal configuration in the active space orbitals. The MRCI energy convergence has been checked by removing the reference state restriction for several species. It was shown that the error was less than 0.5 kcal/mol due to the restriction employed. Further, the symmetry of the electronic orbitals was not exploited. The MOLPRO 2002 program package[20] was used in these electronic structure calculations.

Since it is impossible to carry out direct ab initio dynamics calculations using the MRCI theory because of the prohibitively massive nature of such computations, a variant of the "scaling all correlation" (SAC) method of Truhlar et al.[21−24] is employed. That is, the forces used in classical trajectory propagations are determined by a dual-level ab initio potential energy surface

$$E_{\mathrm{SAC}} = E_{\mathrm{HF}} + \frac{E_{\mathrm{CCD}} - E_{\mathrm{HF}}}{F} \quad (10)$$

where E_{HF} and E_{CCD} are the Hartree−Fock and coupled-cluster with double-excitations energies. The global constant F is a scaling factor for the CCD correlation energy. For a given basis set, this factor should be chosen to balance the correlation energies in all breaking bonds of the system. In the original works of Truhlar et al.,[21−24] the scaling factor was adjusted by fitting the SAC reaction enthalpies to the experimental values. Here this factor was adjusted by minimizing the errors of the relative SAC reaction energies with respect to the relative MRCI reaction energies. The resulting F was found to be 0.78 for the D95(d,p) basis set. The optimal value of F, of course, depends on both the ab initio method used and the basis set, and we selected the D95(d,p) basis after comparing it to several alternative basis sets.

The initial conditions of quasi-classical trajectories (QCT) were sampled in the usual manner[25,26] for a fixed collision energy of 6.8 kcal/mol. The impact parameter and the orientation, rotational energy, and vibrational phases of methane were selected randomly from the appropriate distribution functions. CH_4 was assumed to be in its vibrational ground state. The initial Cartesian coordinates and momenta of the atoms of CH_4 are given by

$$\mathbf{x} = \mathbf{M}^{-1/2}\mathbf{L}\mathbf{Q} + \mathbf{x}_{\mathrm{e}} \quad (11)$$

$$\mathbf{p} = \mathbf{M}^{-1/2}\mathbf{L}\dot{\mathbf{Q}} \quad (12)$$

where $\mathbf{M}$ is a diagonal matrix of atomic masses, $\mathbf{x}_{\mathrm{e}}$ is the equilibrium geometry, and $\mathbf{L}$ is an eigenvector matrix that diagonalizes the mass-weighted Cartesian force constant matrix of CH_4. The ith normal coordinate and its velocity for a given quantum number n_i at $t = 0$ are written as

$$\mathbf{Q}_i = A_i \cos(2\pi\xi_{\mathrm{Q}_i}) \quad (13)$$

$$\dot{\mathbf{Q}}_i = -A_i\lambda_i^{1/2} \sin(2\pi\xi_{\mathrm{Q}_i}) \quad (14)$$

where $A_i = [(2n_i + 1)\hbar/\lambda_i^{1/2}]^{1/2}$ and $\lambda_i^{1/2}$ are the amplitude and frequency of the ith normal mode, and ξ_{Q_i} is a random number uniformly distributed in the interval (0,1). Once the coordinates of CH_4 have been specified, its rotational energies are then added by using a thermal distribution method at $T = 298.0$ K, i.e.,

$$E_{\mathrm{rot}} = 3k_{\mathrm{B}}T/2 = \sum_{\alpha=x,y,z} L_\alpha^{\,2}/2I_\alpha \quad (15)$$

in a principal axis system in which I_α are the inertial moments. The L_α are the components of the total rotational angular momentum, L, and are randomly sampled according to a classical rotor, namely,

$$L_x = L \sin\eta \cos\gamma \quad (16)$$

$$L_y = L \sin\eta \sin\gamma \quad (17)$$

$$L_z = L \cos\eta \quad (18)$$

where the phases are determined by $\cos\eta = 1 - 2\xi_\eta$ and $\gamma = 2\pi\xi_\gamma$ using two additional random numbers uniformly distributed in the interval (0,1). Before the rotational energies are added, the components of the spurious angular momentum $\Sigma_j \mathbf{x}_j \times \mathbf{p}_j$ owing to the vibrational motions are first subtracted from L_α.

Since the above procedure does not consider the anharmonicity of the vibrational motion and the Coriolis coupling, a scaling method was used to adjust the initial momenta and positions of the atoms in CH_4 to obtain an accurate total internal energy as $E^0 = E^0_{\mathrm{vib}} + E^0_{\mathrm{rot}}$. The coordinates and momenta are scaled according to the relations

$$\mathbf{x}_{\mathrm{s}} = (\mathbf{x} - \mathbf{x}_{\mathrm{e}})(E^0/E)^{1/2} + \mathbf{x}_{\mathrm{e}} \quad (19)$$

$$\mathbf{p}_{\mathrm{s}} = \mathbf{p}(E^0/E)^{1/2} \quad (20)$$

where E is the actual internal energy calculated using the exact

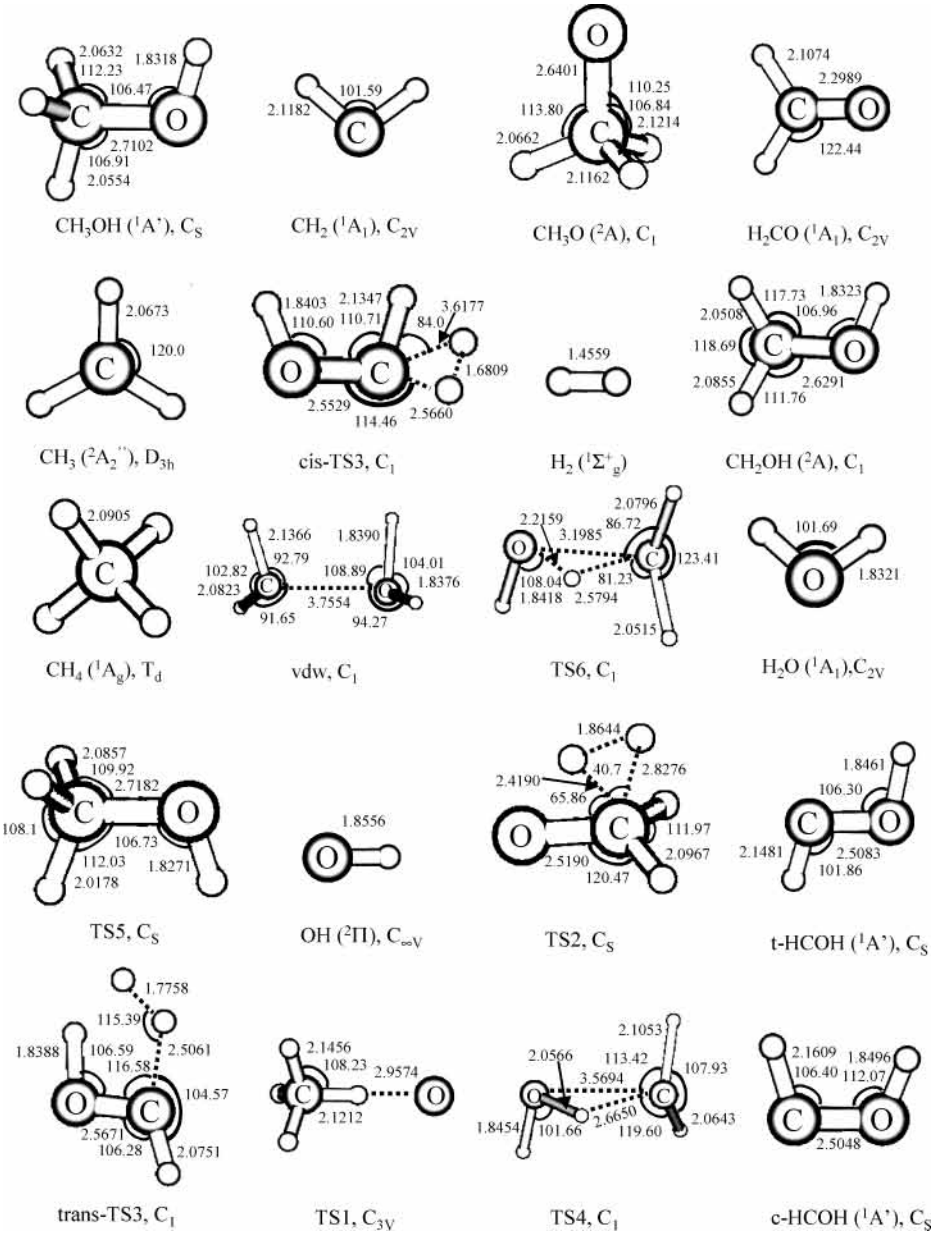

Figure 1. Optimized geometries of stationary points on the potential energy surface of the lowest singlet electronic state of CH_3OH at the CAS-(10,10)/cc-pVDZ level, where lengths and angles are in bohr and degrees, respectively.

Hamiltonian form. The scaling procedure is successively applied until the relative errors are smaller than 0.1%.

The choice of these initial conditions for trajectories is motivated by those of the crossed molecular beam experiment.[11] In the calculations, the maximum impact parameter (b_{max}) and the initial distance (ρ_0) between oxygen and methane are taken to be $b_{max} = 6.0\ a_0$ and $\rho_0 = 10.0\ a_0$, respectively. Hamilton's equations were integrated by the predictor−corrector symplectic reversible integrator of Martyne and Tuckerman[27] with a time step of 0.32 fs. The trajectories were terminated if the distance between two fragments became larger than 7.5 a_0 or the propagation time reached 1.0 ps. The total energy in all trajectories was conserved to better than one percent. All forces used in the dynamics calculations are evaluated using the Gaussian 98 program[28] as

$$\partial E_{SAC}/\partial \mathbf{x}_j = \partial E_{HF}/\partial \mathbf{x}_j + \frac{\partial E_{CCD}/\partial \mathbf{x}_j - \partial E_{HF}/\partial \mathbf{x}_j}{F} \quad (21)$$

The HF and CCD gradient calculations are called by the DualOrthGT dynamics program, which is a quasi-classical trajectory routine for studying unimolecular and bimolecular reactions developed by one of the authors. On a PC−Linux workstation (single 1.7−2.0 GHz P4 Xeon CPU), it took typically nearly 22 h of CPU time to carry out a 1.0 ps trajectory propagation. Therefore, the calculation of the 470 trajectories reported here required in total about 305 days of CPU time. Actually, they were run several at a time (i.e., with trivial parallelization), each on a different processor of a PC cluster.

III. Results and Discussion

III.1. Multireference CI Calculations. The optimized geometries of the stationary points on the CH_3OH potential energy surface are displayed in Figure 1, together with their point group symmetry. Their relative energies and harmonic frequencies are given in Table 1. For the $O(^1D) + CH_4$ reaction, an early transition state (TS1) with a collinear O−H−C geometry is predicted. The classical barrier height obtained is

TABLE 1: Relative MRCI+Q/CBS Energy, Zero-Point Energy (ZPE), and Harmonic Frequencies for the OH + CH_3 System, Where the ZPE and Frequencies Were Calculated at the CAS(10,10)/cc-pVDZ Level[a]

species	energy[b]	ZPE	frequencies /cm[1]
$O(^1D) + CH_4$	0.0 (0.0)	28.00	1354(t), 1571(e), 2970, 3136(t)
$OH + CH_3$	−39.22 (−39.79)	23.93	3613; 580, 1424(e), 3071, 3314(e)
$CH_2(a^1A_1) + H_2O$	−38.75 (−38.96)	23.96	1468, 2868, 3129; 1709, 3734, 3851
$H + CH_3O$	−22.76 (−23.37)	23.10	495, 1030, 1184, 1380, 1501, 1544, 2884, 2940, 3202
$H + CH_2OH$	−31.60 (−31.77)	23.83	460, 811, 1085, 1173, 1409, 1516, 3101, 3319, 3797
H_2 + *trans*-HCOH	−54.44 (−54.06)	22.72	4208; 1105, 1240, 1336, 1532, 2785, 3684
H_2 + *cis*-HCOH	−49.85 (−49.47)	22.31	4208; 1029, 1277, 1333, 1450, 2670, 3636
$H_2 + H_2CO$	−106.40 (−105.56)	22.93	4208; 1209, 1288, 1567, 1795, 2856, 3118
TS1	1.47 (0.90)	27.08	282*i*, 117, 468, 1253, 1332, 1396, 1526, 1535, 2526, 2730, 2777, 3284
TS2	−39.47 (−38.56)	25.87	2374*i*, 924, 927, 1142, 1177, 1204, 1303, 1523, 1652, 2185, 2893, 3169
cis-TS3	−41.06 (−40.66)	25.17	1338*i*, 522, 636, 888, 1112, 1228, 1296, 1454, 1480, 2415, 2866, 3711
trans-TS3	−42.98 (−42.84)	25.48	1419*i*, 516, 602, 951, 1118, 1201, 1318, 1499, 1536, 2138, 3199, 3746
TS4	−47.51 (−47.38)	27.58	1297*i*, 440, 503, 788, 1007, 1132, 1460, 1589, 2337, 3034, 3268, 3731
TS5	−134.26 (−133.33)	31.95	337*i*, 1056, 1098, 1206, 1401, 1483, 1531, 1566, 2949, 3004, 3230, 3832
TS6	−26.79 (−26.06)	27.30	2134*i*, 479, 668, 787, 916, 1224, 1332, 1420, 2030, 3132, 3364, 3746
$CH_2\cdots H_2O$ (vdw)	−48.85 (−49.15)	28.80	124, 241, 546, 582, 941, 1107, 1432, 1690, 2868, 3161, 3733, 3850
CH_3OH	−135.24 (−134.31)	32.37	300, 1065, 1098, 1179, 1425, 1497, 1536, 1551, 2936, 2982, 3280, 3797

[a] Energies in kcal/mol are relative to the $O(^1D) + CH_4$ limit (−115.387393 au). [b] The values in the parentheses are the MRCI+Q/aug-cc-pVTZ//CAS(10,10)/cc-pVDZ energies with respect to the $O(^1D) + CH_4$ limit (−115.345158 au).

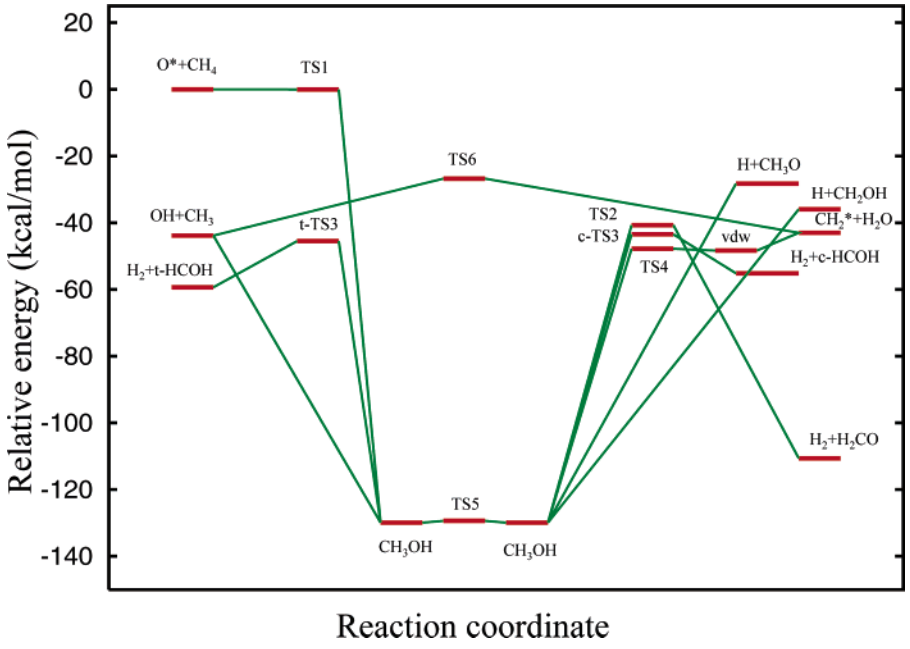

Figure 2. Schematic energy diagram of the $O(^1D) + CH_4$ reaction at the MRCI+Q/CBS level with the zero-point energy correction obtained from the CAS(10,10)/cc-pVDZ results.

1.47 kcal/mol with respect to the $O(^1D) + CH_4$ limit. However, if the zero-point energy is included, the vibrationally adiabatic ground-state barrier height is only 0.56 kcal/mol. This is consistent with the experimental observation[29] of a near zero activation energy for this reaction. It is also in good agreement with the recent CASPT2 result[16] of no barrier in the $O(^1D) + CH_4$ entrance channel. Compared to the previous classical barrier height of 2.1 kcal/mol from MRDCI[12] calculations and 3.6 kcal/mol from PUMP4[13] calculations, the present value of 1.47 kcal/mol is in better accord with experiment.

A schematic energy diagram (including the zero-point energy) for the $O(^1D) + CH_4$ reaction is depicted in Figure 2. The CH_3OH molecule is located at 130.86 kcal/mol below the $O(^1D) + CH_4$ asymptotic limit. This value is comparable to the PUMP4 value of 129.2 kcal/mol.[13] Both are larger than the MRDCI result of 122.2 kcal/mol.[12] Nevertheless, our value is still smaller by 2.8 kcal/mol than the experimental value of 133.7 kcal/mol ($\Delta H^0_{0,K}$).[30] This difference may reflect the maximum errors in this calculation. In addition, a transition state (TS5) is obtained for the internal rotation of the CH_3 moiety around the O−H bond in CH_3OH. The barrier height is only 0.55 kcal/mol with a small imaginary frequency, i.e., 377*i*. Therefore, the O−H torsion mode of CH_3OH can be treated as a hindered rotational motion.

The reaction exothermicity is predicted to be 43.29 kcal/mol for the OH + CH_3 products and 42.79 kcal/mol for the $CH_2(a^1A_1) + H_2O$ products from the $O(^1D) + CH_4$ reactants. These results are in good agreement with the experimental values[30] of 43.6 and 42.8 kcal/mol, respectively. The exothermicity for OH + CH_3 is also in good agreement with the CASPT2 calculation[16] of 42.7 kcal/mol. In addition, the endothermicity of the OH + $CH_3 \rightarrow CH_2(a^1A_1) + H_2O$ reaction is calculated to be 0.50 kcal/mol. Therefore, this MRCI/CASSCF result represents an apparent improvement over the DFT-based results, 4.95 kcal/mol (CCSD(T)//B3LYP)[17] and −1.6 kcal/mol (G2M//B3LYP).[6] This may be because the excited singlet CH_2

TABLE 2: Comparison of Energetics for the $OH + CH_3$ System with Experimental (0 K) and Previous Theoretical Results[a]

species	this work	RMP2[18]	CCI/CAS[4]	MRDCI[12]	G2M[6]	B3LYP[17]	PUMP4[13]	CASPT2[16]	exptl[30]
$OH + CH_3$	0.0	0.0[b]	0.0[b]	0.0	0.0	0.0			0.0
$O(^1D) + CH_4$	43.29			42.5			42.6	42.7	43.6
$CH_2(a^1A_1) + H_2O$	0.50	0.8	0.8		−1.6	4.95			0.8
$H + CH_3O$	15.63			17.9	13.0	12.31	14.6		12.7
$H + CH_2OH$	7.52			11.7	5.0	4.55			4.1
H_2 + *trans*-HCOH	−16.43	−23.1	−17.0		−21.1	−17.63			−17.4
H_2 + *cis*-HCOH	−12.25	−18.2			−17.4				
$H_2 + H_2CO$	−68.18	−77.8	−70.0		−73.8	−70.01			−71.7
TS1	43.85			43.5			42.5		
TS2	1.69	2.3	3.8		−1.3	2.53			
cis-TS3	−0.60				−6.4				
trans-TS3	−2.21	−3.2	−3.1		−3.8	−2.84			
TS4	−4.64	−3.0			−7.8				
TS5	−87.02								
TS6	15.80					16.56			
$CH_2\cdots H_2O$ (vdw)	−4.75	−9.6			−9.2				
CH_3OH	−87.57	−94.2	−88.1	−79.7	−91.9	−88.32	−86.6	−84.8	−90.1

[a] Energies in kcal/mol include the zero-point energy. [b] The $OH + CH_3$ energy is assumed to be 0.8 kcal/mol lower than that of the $CH_2(a^1A_1) + H_2O$ limit in order to make a comparison.

species involved in this reaction is not represented well by a single-determinant wave function.

Furthermore, a van der Waals complex was found for the interaction between H_2 and both *cis*- and *trans*-HCOH molecules. The well depth is predicted to be 0.12 kcal/mol with a distance of 6.709 a_0 from the center of mass of H_2 to the carbon atom in HCOH. If the zero-point energy is included, however, this complex is not stable and consequently is not shown in Figure 2.

For the $OH + CH_3$ reaction, the relative energies of products and transition states are collected in Table 2, together with a comparison with the experimental values[30] and previous theoretical calculations.[4,6,12,17,18] Reactions 2, 3, and 4 are barrierless processes whereas there are transition states in reactions 5, 6, and 7. For reactions 3, 4, and 7 as well as that to form the CH_3OH intermediate, our MRCI/CASSCF results systematically underestimate the reaction enthalpy by about 2.5 to 3.5 kcal/mol compared with the experimental values. The barrier heights of the transition states are generally comparable to the previous ab initio calculations. Notable exceptions are those for the formation of *cis*-HCOH via reaction 6, and TS2 for the formation of H_2CO via reaction 7. The former is higher than the previous theoretical value, while the latter is lower than most of the other theoretical estimates.

It is interesting to examine the $OH + CH_3 \rightarrow CH_2(a^1A_1) + H_2O$ reaction in more detail. Along the minimum energy reaction path, as CH_3OH dissociates to products, there are a late transition state (TS4) and a weakly bound van der Waals complex. Both TS4 and the vdw complex were first studied by Harding et al.[18] using a Møller−Plesset perturbation theory and were subsequently studied by Walch[4] using a CCI/CASSCF method. Our results show that the TS4 transition state lies below the reactant $OH + CH_3$ and the product $CH_2(a^1A_1) + H_2O$ channels. The calculated energy relative to $OH + CH_3$ is −4.64 kcal/mol, which is close to the MP value of −3.0 kcal/mol[18] but smaller than the G2M//B3LYP one of −7.8 kcal/mol.[6] Furthermore, the binding energy of the vdw complex is predicted to be 5.25 kcal/mol with respect to the $CH_2(a^1A_1) + H_2O$ limit. This complex results from electrostatic interactions. Compared with the MP and G2M//B3LYP results,[6,18] the present binding energy is only about half of the previous values. The discrepancy could arise from deficiencies in both the MP and DFT methods that cause the overestimation of the binding energy.

Finally, a transition state (TS6) for the direct $OH + CH_3 \rightarrow CH_2(a^1A_1) + H_2O$ reaction was found. The TS6 lies 15.80 kcal/mol above the $OH + CH_3$ reactant limit, which is in close agreement with the CCSD(T)//B3LYP result of 16.56 kcal/mol.[17] This transition state indicates that the reaction can occur via a hydrogen abstraction mechanism at high temperatures. A contour plot of the potential energy surface for this process is shown in Figure 3.

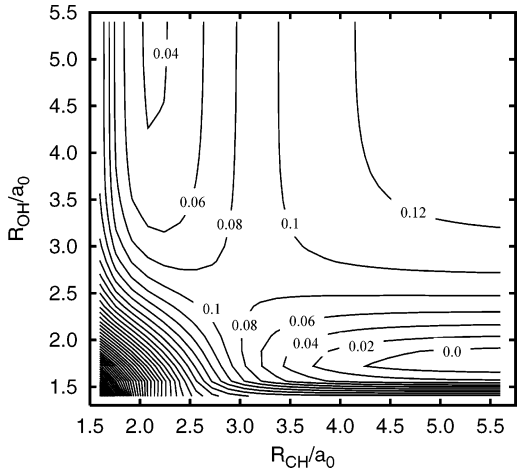

Figure 3. Contour plot for the $OH + CH_3 \rightarrow CH_2(a^1A_1) + H_2O$ reaction calculated at the CAS(10,10)/cc-pVDZ level, where the HO−H′−CH_3 bond is collinear with a HO−H′ bond angle of 108.04° and an HC−H′ bond angle of 86.72°. The geometries of the two fragments OH and CH_3 were fixed at the transition state (TS6) values. The relative contour energies are labeled in hartree.

III.2. Direct ab Initio Dynamics for the $O(^1D) + CH_4$ Reaction. The dynamics study of the $O(^1D) + CH_4$ reaction was performed using the SAC/D95(d,p) method described above. A comparison of the theoretical relative CCD, SAC and MRCI+Q energies at the computed stationary points on the ground-state potential energy surface is given in Table 3. Overall, there is reasonable agreement between the SAC/D95(d,p), MRCI+Q, and the available experimental results. The RMS deviation of the SAC/D95(d,p) relative energies from the MRCI+Q/CBS results at the 16 stationary points listed in the table is only 0.98 kcal/mol. This agreement validates the use of the SAC/D95(d,p) method in the present direct ab initio dynamics calculations, especially because the total energy available to the products of the $O(^1D) + CH_4$ reaction is so large.

In all, 470 trajectories were run at the collision energy of 6.8 kcal/mol. Trajectories that did not dissociate to products within

TABLE 3: Comparison of Theoretical CCD/D95(d,p), SAC/D95(d,p), and MRCI+Q/CBS Energies with the Estimated Experimental Values, Which Are Obtained by Subtracting the Zero-Point Energy (ZPE) Given in Table 1 from the Enthalpies (0 K)[a]

species	E_{CCD}[b]	E_{SAC}[b]	MRCI+Q	exptl[27]
$O(^1D) + CH_4$	0.0	0.0	0.0	0.0
$OH + CH_3$	−45.11	−40.90	−39.22	−39.53
$CH_2(a^1A_1) + H_2O$	−36.41	−38.63	−38.75	−38.76
$H + CH_3O$	−27.11	−23.48	−22.76	−26.0
$H + CH_2OH$	−32.86	−31.87	−31.60	−35.33
H_2 + *trans*-HCOH	−53.65	−57.56	−54.44	−55.72
H_2 + *cis*-HCOH	−48.21	−52.19	−49.85	
$H_2 + H_2CO$	−105.42	−110.60	−106.40	−110.23
TS1	0.02	−0.12	1.47	
TS2	−30.66	−37.32	−39.47	
cis-TS3	−35.34	−41.33	−41.06	
trans-TS3	−38.56	−44.62	−42.98	
TS4	−42.77	−48.62	−47.51	
TS5	−133.12	−137.86	−134.26	
TS6	−17.83	−24.91	−26.79	
$CH_2\cdots H_2O$ (vdw)	−48.03	−51.97	−48.85	
CH_3OH	−134.40	−139.15	−135.24	−138.07

[a] Energies in kcal/mol are relative to the $O(^1D) + CH_4$ limit. [b] Energies at the $O(^1D) + CH_4$ limit are −115.213388 au for CCD/D95(d,p), and −115.305 683 au for SAC/D95(d,p), respectively.

TABLE 4: Product Distributions of 470 Trajectories at 1.0 ps for the $O(^1D) + CH_4$ Collision with a Translational Energy of 6.8 kcal/mol[a]

species	trajectory no.	direct	complex	product fraction
$O(^1D) + CH_4$	70			
$OH + CH_3$	56	0.1400	0.5899	0.7299
$CH_2(a^1A_1) + H_2O$	25	0.0625	0.0023	0.0648
$H + CH_3O$	47	0.1175	0.0003	0.1178
$H + CH_2OH$	6	0.0150	0.0398	0.0548
H_2 + *trans*-HCOH	2	0.0050	0.0082	0.0132
H_2 + *cis*-HCOH	0	0.0	0.0031	0.0031
$H_2 + H_2CO$	3	0.0075	0.0014	0.0089
$H + H + H_2CO$	3	0.0075	0.0	0.0075
CH_3OH^* (complex)	258			

[a] The final product fraction was calculated by adding the contributions from the unimolecular dissociation of the complex CH_3OH^*. The contributions from the direct and complex reactions are given in the last two columns.

1.0 ps of simulated time were terminated and counted as forming the intermediate complex CH_3OH^*. We arbitrarily chose this 1.0 ps criterion because it is longer than the rotational period of the excited intermediate complex, and we assume that collision complexes living longer than 1.0 ps will dissociate statistically. We found that direct reactions normally occurred within 450 fs so that it was not difficult to distinguish them form the long-lived trajectories, and no effort was made to distinguish the lifetime of the collision complexes from the simulated time of the trajectory. The results obtained are presented in Table 4, and the opacity function for the total reaction probability is shown in Figure 5a. The total reaction cross section was calculated to be $89.8 \pm 3.2\ a_0^2$. Although the reaction probability at the maximum impact parameter $b_{max} = 6.0\ a_0$ does not clearly show zero probability in Figure 5a, no reactive trajectory was found in an ensemble of 15 test trajectories with $b_{max} = 6.0\ a_0$. Therefore, the truncation errors for the cross sections by using this maximum impact parameter should be within the statistical error bars.

The dissociation of the intermediate complex CH_3OH^* remaining after 1.0 ps is treated using a statistical theory. In such a way, we can roughly distinguish a direct reaction mechanism from reactions via a long-lived complex. The final reaction probability P_j^r is calculated by the sum of these two contributions as

$$P_j^r = P_j^d + P_c^* f_j \tag{22}$$

where $P_j^d = N_j^d/N_{total}$ is the direct reaction probability for the product channel j at a time less than 1.0 ps; and $P_c^* = N_c^*/N_{total}$ is the probability of forming the intermediate complex CH_3OH^* at the time of 1.0 ps. Here N_{total}, N_j^d and N_c^* are the numbers of total trajectories, of direct reactions resulting in channel j, and of complex-forming trajectories, respectively, and f_j is the branching fraction from the unimolecular dissociation of CH_3OH^*. It is calculated using RRKM theory as[31,32]

$$f_j = \frac{\sigma_j N_j(E - E_j^{\ddagger})}{\sum_k \sigma_k N_k(E - E_k^{\ddagger})} \tag{23}$$

where σ_j and $N_j(E)$ are the reaction degeneracy and the sum of the states for the channel j. In this work, the sums of the states are evaluated using the saddle-point method with the harmonic-oscillator and rigid-rotor approximations. For the barrierless product channels, they are determined using a variational RRKM method[33,34] by minimizing the quantity

$$\frac{\partial N_j(E - E_j^{\ddagger};R_j)}{\partial R_j} = 0 \tag{24}$$

where R_j is the reaction coordinate corresponding to the breaking bond. The interaction potentials $V(R)$ along the reaction path were calculated using the B3LYP/6-31G(d,p) theory with the intrinsic reaction coordinate (IRC) method in Gaussian 98. The vibrational frequencies perpendicular to the reaction coordinate were projected using a "Freq = projected" option. Finally, the sums of states are calculated using the convolution integral

$$N(E) = \int_0^E N_{vib}(E - \epsilon;R)\rho_{rot}(\epsilon;R)\, d\epsilon \tag{25}$$

with $N_{vib} = E^k/k!\Pi h\nu_j$ for the sum of vibrational states of k harmonic oscillators, and $\rho_{rot} = 2\sqrt{E/B_A B_B B_C}$ for the density of rotational states. Here B_β are the rotational constants of the system. In eq 25 the R-dependence applies only for the barrierless processes. Especially, for the $OH + CH_3$ channel, if the two lowest vibrational frequencies are smaller than 100 cm^{-1}, they are treated as a two-dimensional free-rotor with a density of states of $\rho(E) = 2/h\sqrt{\nu_1\nu_2}$. With these classical limit treatments, the integral in eq 25 can be easily evaluated. Since the total energy is large (for instance, more than 50 kcal/mol for $OH + CH_3$) in this case, such an approximation should be sufficiently accurate.

The branching fractions are predicted to be 0.725:0.186:0.025:0.064 into the product channels OH, H, H_2, and H_2O, respectively. They are in excellent agreement with the experimental values.[9,35,36] Lin et al.[36] recommended the branching fractions as 0.69:0.23:0.05:0.015 according to their crossed-beam experiments. Satyapal and co-workers[35] obtained branching fractions of 0.75:0.25 for the OH and H channels. Obviously, the main products are $OH + CH_3$. Although the major portion (about 81%) of the OH yield is produced via a long-lived complex, a substantial portion of the OH product is produced via a direct reaction mechanism. Trajectories show that these direct reactions proceed by a process of $O(^1D)$ inserting into a C−H bond of CH_4 rather than directly abstracting or stripping off a hydrogen atom from methane. One

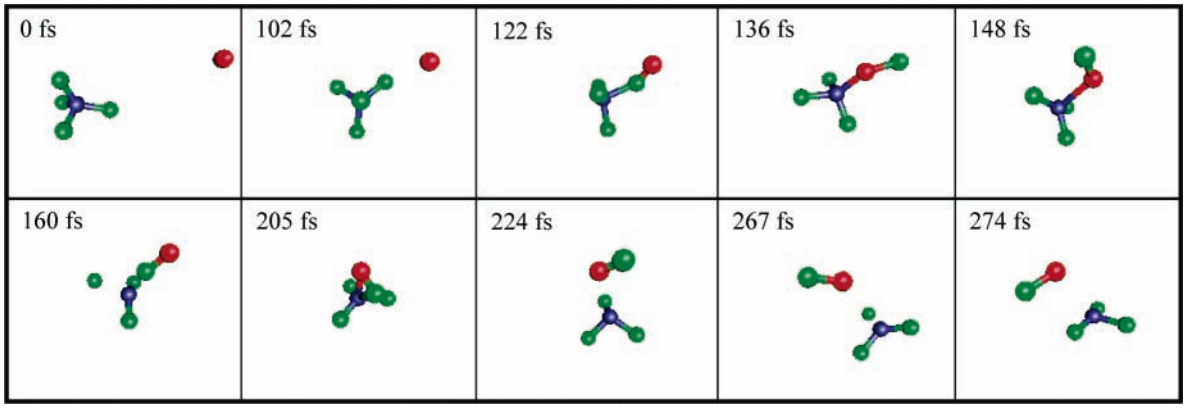

Figure 4. A trajectory for the formation of $OH + CH_3$ via a direct reaction pathway. The time in femtoseconds is indicated in each panel.

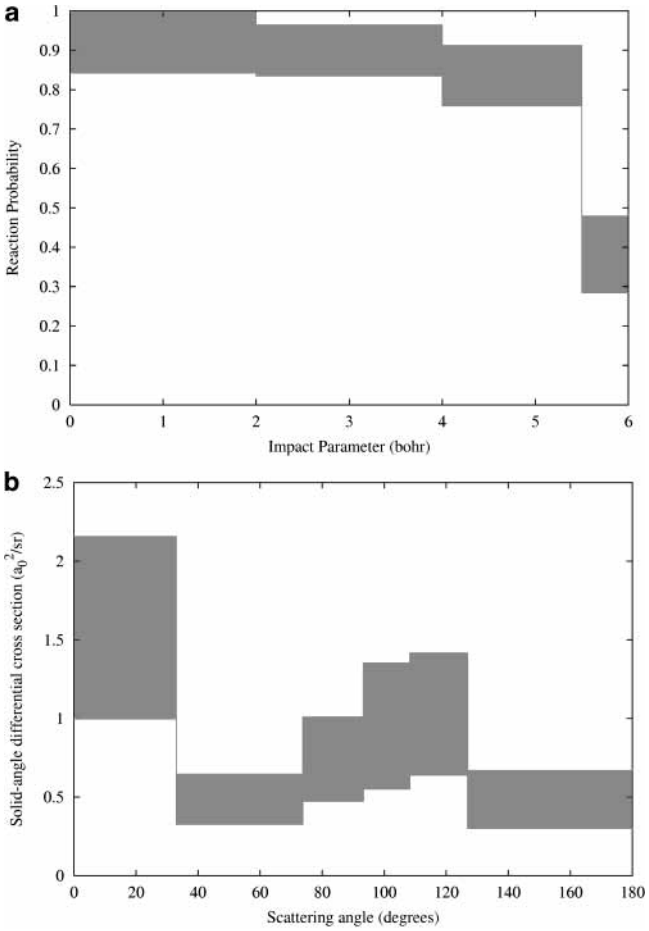

Figure 5. (a) Calculated opacity function for the total reaction probability and (b) calculated differential cross section for the $O(^1D) + CH_4 \rightarrow OH + CH_3$ reaction via the insertion direct mechanism, where zero degrees corresponds to forward scattering. The maximum observed impact parameter for a reactive collision was 5.92 a_0. The shaded boxes indicate the function values ± one standard deviation for each bin along the abscissa.

such typical trajectory is displayed in Figure 4 as a function of time. The insertion of the oxygen atom into the C−H bond occurs around 135 fs. Although there is an energized CH_3OH^* molecule formed, the lifetime of this intermediate is only 120 fs. As a result, this is considered to be a direct reaction process. Therefore, our dynamics results demonstrate multiple pathways for the $O(^1D) + CH_4 \rightarrow OH + CH_3$ reaction, which is consistent with the crossed molecular beam study[11] as well as the previous QCT calculations.[14] The direct reaction mechanism also implies that the OH rovibrational state distributions could be nonstatistical as observed by several experimental groups.[34−43] Unfortunately, the number of such reactive trajectories is too small to permit a quantitative analysis of the product distributions. More importantly, most of the reactive trajectories were terminated before the products had reached their asymptotic values of relative velocity and internal energy.

The calculated differential cross section[44,45] for the direct component of the $O(^1D) + CH_4 \rightarrow OH + CH_3$ reaction is displayed in Figure 5b. It is clearly seen despite a rather large statistical uncertainty that the differential cross section for the direct reaction exhibits a pronounced forward peak superimposed on a relatively isotropic background. This conclusion is coincident with most recent crossed-beam observations.[11] Again, it is not necessary to use a stripping mechanism to explain the forward scattering for this reaction. Recently, Gonzalez and coworkers[15] reported a reduced-dimensional QCT study using a pseudotriatomic model. At a similar collision energy (6.5 kcal/mol), the probability of abstraction reactions is negligible, i.e., near 0.0009. In particular, they also concluded that the total differential cross sections show forward and backward peaks. Therefore, our outcomes are in excellent agreement regardless of the number of the dynamical degrees-of-freedom treated.

It was found that the products CH_3O and H_2O are produced mainly via a direct mechanism, whereas the product CH_2OH is largely formed via the intermediate complex. Interestingly, in addition to the unimolecular dissociation of CH_3OH^*, there are three direct reaction mechanisms for the formation of H_2CO. They are the elimination of H_2, the elimination of two hydrogen atoms, and the elimination of two hydrogen atoms via the secondary reaction $H + CH_3O \rightarrow H + H + H_2CO$. These trajectories are shown in Figure 6. They provide concrete evidence that the product CH_3O can further dissociate to smaller fragments as shown in Figure 6c. In other words, for the $O(^1D) + CH_4$ reaction, secondary reactions are also important, especially for the H channel.

By using the reaction probability, we can estimate the rate constant at this collision energy as $k_E = gV_T\sigma_r = 1.34 \times 10^{-10}$ cm^3 molecule^{-1} s^{-1}, where $g = {}^1/_5$ is the electronic degeneracy factor of $O(^1D)$. Here V_T and σ_r are the collision velocity and the reaction cross section, respectively. This value is comparable to the recommended thermal rate constant (300 K)[46] of 1.5×10^{-10} cm^3 molecule^{-1} s^{-1}. For the $O(^1D) + CH_4$ reaction, the thermal rate constant is weakly temperature dependent,[17] varying as $T^{1/6}$.

IV. Summary

The potential energy surface for the $O(^1D) + CH_4$ and $OH + CH_3$ reactions has been characterized using the restricted

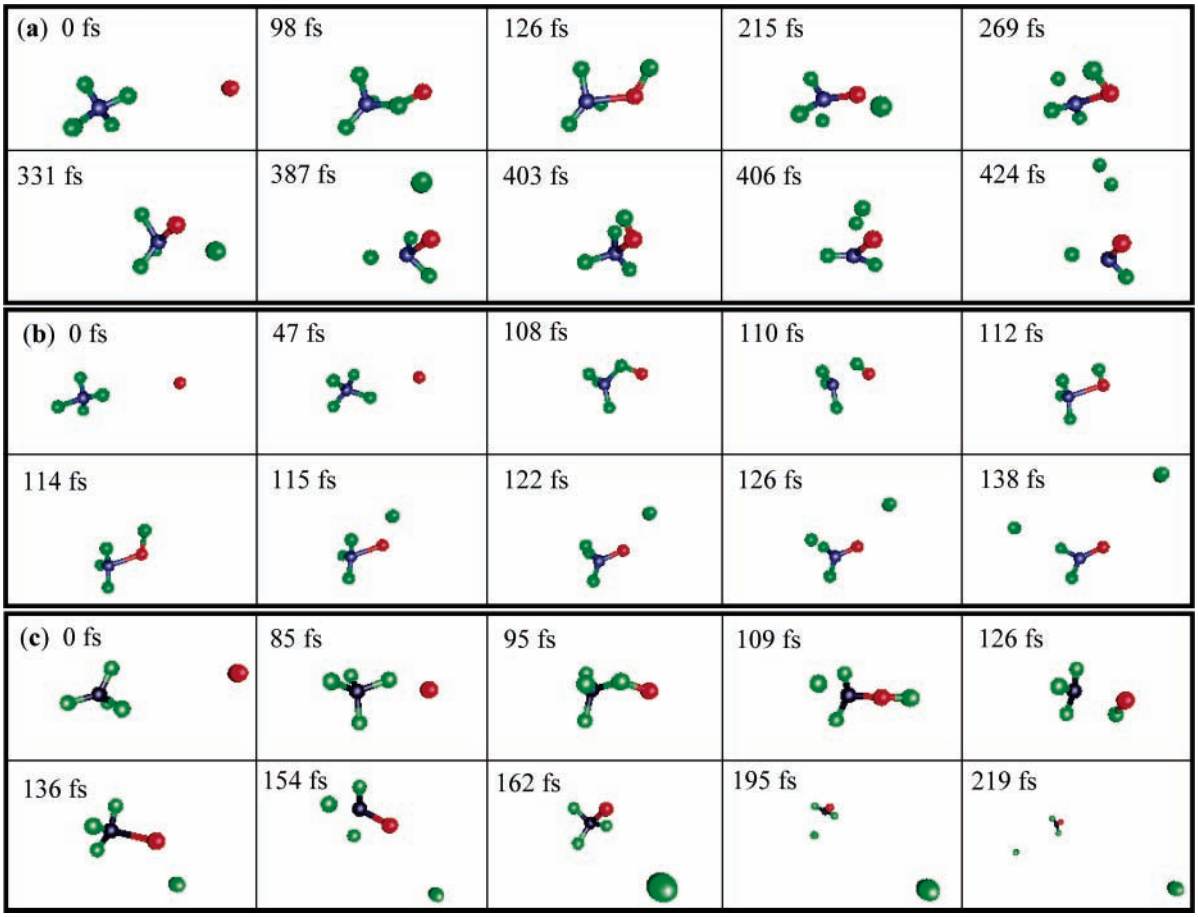

Figure 6. Three typical trajectories for the formation of H_2CO: (a) $O(^1D) + CH_4 \rightarrow H_2 + H_2CO$, (b) $O(^1D) + CH_4 \rightarrow 2H + H_2CO$, and (c) $O(^1D) + CH_4 \rightarrow H + H_3CO \rightarrow 2H + H_2CO$, where the time in femtoseconds is indicated in each panel.

MRCI+Q/aug-cc-pVTZ//CAS(10,10)/cc-pVDZ method extrapolated to the complete basis set limit. A small early barrier with a classical barrier height of 1.47 kcal/mol is determined for the $O(^1D) + CH_4$ reaction. If the zero-point energy correction is included, the vibrationally adiabatic ground-state barrier height is 0.56 kcal/mol. The exothermicity (0 K) of the major reaction $O(^1D) + CH_4 \rightarrow OH + CH_3$ is predicted to be 43.29 kcal/mol. The endothermicity of another key reaction, $OH + CH_3 \rightarrow CH_2(a^1A_1) + H_2O$, is obtained as 0.50 kcal/mol. Both results are in good agreement with the experimental values. However, the calculated enthalpies for the CH_3OH molecule and the H and H_2 product channels are systematically underestimated by about 1.0 to 3.5 kcal/mol.

Along the minimum energy reaction path of the $OH + CH_3 \rightarrow CH_2(a^1A_1) + H_2O$ reaction, as CH_3OH dissociates to products, there are a late transition state (TS4) and a van der Waals complex. Their energies (including the zero-point energy correction) are obtained as −5.14 kcal/mol and −5.25 kcal/mol, respectively, with respect to the $CH_2(a^1A_1) + H_2O$ asymptote. Furthermore, it was also noticed that this reaction could occur via a direct abstraction mechanism through the TS6 transition state at high temperatures. The vibrationally adiabatic ground-state barrier height is predicted to be 15.8 kcal/mol. Nevertheless, this barrier height is much higher than the transition state (6.7 kcal/mol)[47] on the triplet potential energy surface for the $OH + CH_3$ reaction.

Finally, a direct ab initio dynamics study has been performed for the $O(^1D) + CH_4$ reaction at a collision energy of 6.8 kcal/mol. The products are dominated by the OH and H channels. In particular, three direct mechanisms have been found for the formation of H_2CO, one of which also indicates that a secondary reaction corresponding to the unimolecular dissociation of CH_3O is involved. Further, it was noticed that the direct reactions for the products OH and CH_3 proceed through an insertion mechanism to form a very short-lived vibrationally excited CH_3OH^* molecule. These reactions are preferentially forward scattered, in good agreement with the crossed molecular beam experiments[11] as well as the pseudotriatomic QCT calculations.[14,15] In this study, only the lowest singlet electronic state was considered. Quite recently, CASSCF and CASPT2 calculations[16] have indicated that the barrier height for the $O(^1D) + CH_4 \rightarrow OH + CH_3$ reaction is around 1.2−12.0 kcal/mol on the first excited singlet state. This result conflicts with the high barrier that was predicted previously.[12] Nevertheless, the reactivity on this excited state would be expected to be much smaller than that on the ground-state surface, as the latter is nearly barrierless and quite isotropic in the entrance channel.[16]

Acknowledgment. This work was performed at Brookhaven National Laboratory under Contract No. DE-AC02-98CH10886 with the U.S. Department of Energy and supported by its Division of Chemical Sciences, Office of Basic Energy Sciences. H.G.Y. was partially supported by a Goldhaber Fellowship.

References and Notes

(1) Hack, W.; Wagner, H. G.; Wilms, A. *Ber. Bunsen-Ges. Phys. Chem.* **1988**, *92*, 620.

(2) Carstensen, H. H.; Wagner, H. G. *Ber. Bunsen-Ges. Phys. Chem.* **1995**, *99*, 1539.

(3) Deters, R.; Otting, M.; Wagner, H. G.; Temps, F.; Laszlo, B.; Dobe, S.; Berces, T. *Ber. Bunsen-Ges. Phys. Chem.* **1998**, *102*, 58.

(4) Walch, S. P. *J. Chem. Phys.* **1993**, *98*, 3163.

(5) Walch, S. P. *J. Chem. Phys.* **1993**, *98*, 3076.

(6) Xia, W. S.; Zhu, R. S.; Lin, M. C.; Mebel, A. M. *Faraday Discuss.* **2001**, *119*, 191.
(7) Dean, A. M.; Westmoreland, P. R. *Int. J. Chem. Kinet.* **1987**, *19*, 207.
(8) Avillez, R. De. A.; Baulch, D. L.; Pilling, M. J.; Robertson, S. H.; Zeng, G. *J. Phys. Chem. A* **1997**, *101*, 9681.
(9) Miller, C. C.; Van Zee, R. D.; Stephenson, J. C. *J. Chem. Phys.* **2001**, *114*, 1214.
(10) Gonzalez, M.; Puyuelo, M. P.; Hernando, J.; Sayos, R.; Enriquez, P. A.; Guallar, J.; Banos, I. *J. Phys. Chem. A* **2000**, *104*, 521.
(11) Lin, J. J.; Shu, J.; Lee, Y. T.; Yang, X. *J. Chem. Phys*. **2000**, *113*, 5287.
(12) Arai, H.; Kato, S.; Koda, S. *J. Phys. Chem.* **1994**, *98*, 12.
(13) Gonzalez, M.; Hernando, J.; Banos, I.; Sayos, R. *J. Chem. Phys*. **1999**, *111*, 8913.
(14) Gonzalez, M.; Hernando, J., Puyuelo, M. P.; Sayos, R. *J. Chem. Phys.* **2000**, *113*, 6748.
(15) Sayos, R.; Hernando, J., Puyuelo, M. P.; Enriquez, P. A., Gonzalez, M. *Phys. Chem. Chem. Phys.* **2002**, *4*, 288.
(16) Hernando, J.; Millán, J.; Sayós, R.; González, M. *J. Chem. Phys.* **2003**, *119*, 9504.
(17) Chang, A. H. H.; Lin, S. H. *Chem. Phys. Lett*. **2002**, *363*, 175.
(18) Harding, L. B.; Schlegel, H. B.; Krishnan, R.; Pople, J. A. *J. Phys. Chem.* **1980**, *84*, 3394.
(19) Halkier, A.; Helgaker, T.; Jorgensen, P.; Klopper, W.; Koch, H.; Olsen, J.; Wilson, A. K. *Chem. Phys. Lett*. **1998**, *286*, 243.
(20) MOLPRO is a package of ab initio programs written by Werner, H.-J.; Knowles, P. J. with contributions from R. D. Amos, A. Bernhardsson, A. Berning, P. Celani, D. L. Cooper, M. J. O. Deegan, A. J. Dobbyn, F. Eckert, C. Hampel, G. Hetzer, T. Korona, R. Lindh, A. W. Lloyd, S. J. McNicholas, F. R. Manby, W. Meyer, M. E. Mura, A. Nicklass, P. Palmieri, R. Pitzer, G. Rauhut, M. Schutz, H. Stoll, A. J. Stone, R. Tarroni, and T. Thorsteinsson.
(21) Gordon, M. S.; Truhlar, D. G. *J. Am. Chem. Soc*. **1986**, *108*, 5412.
(22) Gordon, M. S.; Truhlar, D. G. *Int. J. Quantum Chem.* **1987**, *31*, 81.
(23) Gordon, M. S.; Nguyen, K. A.; Truhlar, D. G. *J. Phys. Chem.* **1989**, *93*, 7356.
(24) Gao, J.; Thompson, M. A., Eds. *Combined Quantum Mechanical and Molecular Mechanical Methods*; American Chemical Society: Washington, DC, 1998.
(25) Hase, W. L. In *Encyclopedia of Computational Chemistry*; Schleyer, P. von R, Ed.; John Wiley & Sons: New York, 1998.
(26) Billing, G. D.; Mikkelsen, K. V. *Advanced Molecular Dynamics and Chemical Kinetics*; Wiley Europe: New York, 1997.
(27) Martyne, G. J.; Tuckerman, M. E. *J. Chem. Phys.* **1995**, *102*, 8071.
(28) Frisch, M. J.; Trucks, G. W.; Schlegel, H. B.; Scuseria, G. E.; Robb, M. A.; Cheeseman, J. R.; Zakrzewski, V. G.; Montgomery, J. A., Jr.; Stratmann, R. E.; Burant, J. C.; Dapprich, S.; Millam, J. M.; Daniels, A. D.; Kudin, K. N.; Strain, M. C.; Farkas, O.; Tomasi, J.; Barone, V.; Cossi, M.; Cammi, R.; Mennucci, B.; Pomelli, C.; Adamo, C.; Clifford, S.; Ochterski, J.; Petersson, G. A.; Ayala, P. Y.; Cui, Q.; Morokuma, K.; Malick, D. K.; Rabuck, A. D.; Raghavachari, K.; Foresman, J. B.; Cioslowski, J.; Ortiz, J. V.; Stefanov, B. B.; Liu, G.; Liashenko, A.; Piskorz, P.; Komaromi, I.; Gomperts, R.; Martin, R. L.; Fox, D. J.; Keith, T.; Al-Laham, M. A.; Peng, C. Y.; Nanayakkara, A.; Gonzalez, C.; Challacombe, M.; Gill, P. M. W.; Johnson, B. G.; Chen, W.; Wong, M. W.; Andres, J. L.; Head-Gordon, M.; Replogle, E. S.; Pople, J. A. *Gaussian 98*, revision A.7; Gaussian, Inc.: Pittsburgh, PA, 1998.
(29) Atkinson, R.; Baulch, D. L.; Cox, R. A.; Hampson, R. F., Jr.; Kerr, J. A.; Troe, J. *J. Phys. Chem. Ref. Data* **1992**, *21*, 1215.
(30) Chase, W. W., Jr.; Davies, C. A.; Downey, R., Jr.;.; Frurip, D. J.; McDonald, R. A.; Syverud, A. N. *J. Phys. Chem. Ref. Data, Suppl. 1*, **1985**, *14*.
(31) Baer, T.; Hase, W. L. *Unimolecular Reaction Dynamics: Theory and Experiments*; Oxford University Press: New York, 1996.
(32) Weston, R., Jr.; Schwarz, H. A. *Chemical Kinetics*; Prentice-Hall: NJ, 1972.
(33) Marcus, R. A. *Chem. Phys. Lett.* **1988**, *144*, 208.
(34) Hase, W. L. *Acc. Chem. Res.* **1983**, *16*, 258.
(35) Satyapal, S.; Park, J.; Bersohn, R.; Katz, B. *J. Chem. Phys.* **1989**, *91*, 6873.
(36) Lin, J. J.; Harich, S.; Lee, Y. T.; Yang, X. *J. Chem. Phys.* **1999**, *110*, 10821.
(37) Luntz, A. C. *J. Chem. Phys*. **1980**, *73*, 1143.
(38) Cheskis, S. G.; Iogansen, A. A.; Kulakov, P. V.; Razuvaev, I. Y.; Sarkissov, O. M.; Titov, A. A. *Chem. Phys. Lett*. **1989**, *155*, 37.
(39) Park, C. R.; Wiesenfeld, J. R. *J. Chem. Phys.* **1991**, *95*, 8166.
(40) Aker, P. M.; OBrien, J. J. A.; Sloan, J. J. *J. Chem. Phys.* **1986**, *84*, 745.
(41) Suzuki, T.; Hirota, E. *J. Chem. Phys.* **1993**, *98*, 2387.
(42) Schott, R.; Schluter, J.; Kleinermanns, K. *J. Chem. Phys*. **1995**, *102*, 8371.
(43) Schluter, J.; Schott, R.; Kleinermanns, K. *Chem. Phys. Lett*. **1993**, *213*, 262.
(44) Faist, M. B.; Muckerman, J. T.; Schubert, F. E. *J. Chem. Phys.* **1978**, *69*, 4087.
(45) Muckerman, J. T.; Faist, M. B. *J. Phys. Chem.* **1979**, *83*, 79.
(46) Atkinson, R.; Baulch, D. L.; Cox, R. A.; Hampson, R. F., Jr.; Kerr, J. A.; Troe, J. *J. Phys. Chem. Ref. Data* **1992**, *21*, 1125.
(47) Wilson, C.; Balint-Kurti, G. G. *J. Phys. Chem. A* **1998**, *102*, 1625.